Piperidine based 1,2,3-triazolylacetamide derivatives induce cell cycle arrest and apoptotic cell death in *Candida auris*

Vartika Srivastava [a], Mohmmad Younus Wani [b,*], Abdullah Saad Al-Bogami [b], Aijaz Ahmad [a,c,*]

[a] *Clinical Microbiology and Infectious Diseases, School of Pathology, Faculty of Health Sciences, University of the Witwatersrand, Johannesburg 2193, South Africa*
[b] *University of Jeddah, College of Science, Department of Chemistry, Jeddah 21589, Saudi Arabia*
[c] *Infection Control Unit, Charlotte Maxeke Johannesburg Academic Hospital, National Health Laboratory Service, Johannesburg 2193, South Africa*

GRAPHICAL ABSTRACT
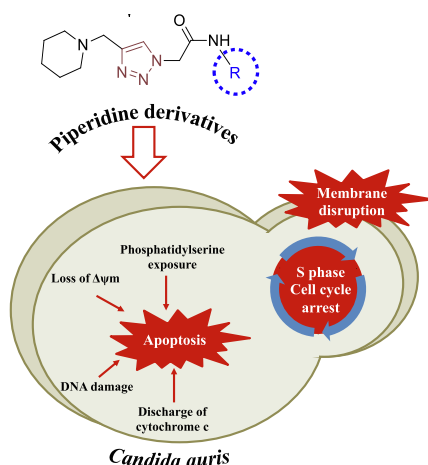
ARTICLE INFO

ABSTRACT

Introduction: The fungal pathogen *Candida auris*, is a serious threat to public health and is associated with bloodstream infections causing high mortality particularly in patients with serious medical problems. As this pathogen is generally resistant to all the available classes of antifungals, there is a constant demand for novel antifungal drugs with new mechanisms of antifungal action.

Objective: Therefore, in this study we synthesised six novel piperidine based 1,2,3-triazolylacetamide derivatives (pta1-pta6) and tested their antifungal activity and mechanism of action against clinical **C. auris** isolates.

Methods: Antifungal susceptibility testing was done to estimate MIC values of piperidine derivatives following CLSI recommended guidelines. MUSE Cell Analyzer was used to check cell viability and cell cycle arrest in *C. auris* after exposure to piperidine derivatives using different kits. Additionally, fluorescence microscopy was done to check the effect of test compound on *C. auris* membrane integrity and related apoptotic assays were performed to confirm cellular apoptosis using different apoptosis markers.

Results: Out of the six derivatives; pta1, pta2 and pta3 showed highest active with MIC values from 0.24 to 0.97 µg/mL and MFC ranging from 0.97 to 3.9 µg/mL. Fungicidal behaviour of these compounds

was confirmed by cell count and viability assay. Exposure to test compounds at sub-inhibitory and inhibitory concentrations resulted in disruption of *C. auris* plasma membrane. Further in-depth studies showed that these derivatives were able to induce apoptosis and cell cycle arrest in S-phase. Furthermore, the compounds demonstrated lower toxicity profile.

Conclusion: Present study suggests that the novel derivatives (pta1-pta3) induce apoptotic cell death and cell cycle arrest in *C. auris* and could be potential candidates against *C. auris* infections.

Introduction

Candida auris, a pathogenic yeast bearing superbug-like characteristics, is causing invasive outbreaks around the globe. This species of *Candida* is frequently reported to be multidrug resistant (MDR) and can persist in nosocomial environment due to its high tolerance to antiseptics and disinfectants. At present, 33 countries from 6 continents have been affected by *C. auris* infections with crude mortality of around 30–72% [1]. In year 2014, the first case was reported in South Africa and between year 2012 and 2016 around 1700 positive cases were reported [1]. The principal reason behind this rapid spread in nosocomial environment is considered to be its capability to form biofilms on polymeric surfaces of medical devices [2].

Most *C. auris* infections are azole resistant and are mostly treatable with echinocandins. However, according to recent studies higher minimum inhibitory concentrations (MICs) values against all available antifungal drugs have been demonstrated by some *C. auris* isolates [3]. This indicates that management strategies for this pan-resistant species would be highly difficult and therefore, there is an undeniable demand for new antifungal molecules with novel and alternative modes of action against *C. auris*. Development of new antifungal therapies is definitely an uphill and challenging task because of the many similarities between fungal and human cells. An effective and interim strategy to tackle this multidrug resistant menace has been the structural modification of the known antifungal drug classes, and it has greatly helped evading and fudging the fungal drug resistance mechanisms [4,5].

Azoles are the most widely used fungistatic and extremely well tolerated drugs that interfere with the ergosterol biosynthesis, causing membrane disruption. Their extended and protracted use in absence of any alternatives has enormous contribution in drug resistance development in *Candida*. Despite similar mechanism of action, the structural differences in different triazoles have led to huge difference in their pharmacokinetic properties including metabolism and elimination. Any changes in the chemical structures of this class of drugs, therefore, would give a promising scaffold with distinct pharmacokinetic properties that could be used to combat the multidrug resistance problem, at least, until a new drug class arrives.

Triazoles have been the backbone of first- and second-generation azole antifungals and have been used as frontline drugs for the treatment and prophylaxis of many systemic fungal infections [6,7]. The piperidine ring is also an extremely important building block and the most commonly used heterocycle among US FDA approved pharmaceuticals [8]. Synthesis of piperidine derivatives has become popular among organic chemists, as they are important core for various pharmaceuticals, agrochemicals and natural products [9]. The commonly prescribed drugs with piperidine nucleus are, nesina (oral anti-diabetic drug), methylphenidate (improved concentration in children), risperdal (reduce bipolar disorder, schizophrenia), tofacitinib (treat autoimmune diseases) [10]. Additionally, triazole derivatives have been well established to possess different therapeutic activity, namely, antimicrobial, antitumor, antiviral, antimalarial, anti-tubercular,

anti-leishmanial, antidiabetic, and neuroprotective agents [11]. Anti-*Candida* activity, mostly against *C. albicans*, of piperidine derivatives has also been reported [12,13]. Triazoles linked with some other pharmacophoric moieties have already shown promise as important scaffolds with interesting biological activities [14–19]. Therefore, in this study we synthesized six novel piperidine derivatives containing a triazole moiety flanked with an acetamide functionality and tested them against different clinical isolates of *C. auris* for their antifungal activity. For insight studies, we also tested their mode of antifungal action by studying physiology of cell death and cell cycle analysis.

Materials and method

Chemistry

Experimental

The chemical reagents and solvents were procured from Sigma Aldrich and Merck Germany. TLC plates used were precoated aluminium sheets (silica gel 60 F254, Merck Germany) and visualization was done by UV light in a UV cabinet. Heraeus Vario EL III analyser was used for elemental analysis. Bruker ALPHA FTIR spectrometer (Eco-ATR) was used for FTIR analysis. Bruker AVANCE 400 spectrometer was used for ^{1}H NMR (400 MHz, DMSO d_6) (δ ppm) and ^{13}C NMR (100 MHz, DMSO d_6) with TMS (Tetramethyl silane) as standard. ESI-MS positive ion mode was recorded on Micromass Quattro II triple quadrupole mass spectrometer.

Click synthesis of 2-(4-(piperidin-1-ylmethyl)-1H-1,2,3-triazol-1-yl) acetic acid (3)

Compound **3** (*2-(4-(piperidin-1-ylmethyl)-1H-1,2,3-triazol-1-yl) acetic acid*) was obtained through a click chemistry reaction of (1-(prop-2-yn-1-yl)Piperidine) **(2)** with 2-azidoaceticacid in equimolar ratio in DMF. Compound **(2)** in turn was obtained by treating piperidine (1 g, 11.74 mmol) in dry acetone with propargyl bromide dropwise (1.5 g) at room temperature, resulting in precipitation of the product in acetone immediately. The product was filtered, washed, dried and used as such in the next reaction.

Yield: 98%; Anal. Calc. For $C_{10}H_{16}N_4O_2$: C 53.56, H 7.19, N 24.98%; found: C 53.70, H 7.26, N 24.85%; FTIR ν_{max} cm^{-1}: 3265 (—OH str), 3185 (C—H triazole ring), 2860 (C—H), 1760 (C=O); ^{1}H NMR (DMSO d_6) δ (ppm): 9.26 (1H, s, OH), 7.55 (1H, s, triazole ring), 4.92 (2H, s, CH$_2$,), 3.70 (2H, s, CH$_2$), 2.63 (2H, t; *J* = 4 Hz), 2.36 (2H, t; *J* = 4 Hz), 1.66–1.58 (6H, m); ^{13}C NMR (DMSO d_6) δ (ppm): 170.8 (C=O), 154.82, 146.0, 122.8, 61.7, 54.6, 48.9, 27.0, 25.2; ESI-MS *m*/*z*: [M$^+$+H] 225.12; calculated: 224.13.

Synthesis of piperidine based 1,2,3-triazolylacetamide derivatives (pta1-pta6)

The target derivatives **(pta1-pta6)** were synthesized following a straight forward synthetic route as shown in Scheme 1. Compound **3** (1.0 mmol) on treatment with different amines (1.1 mmol) in presence of coupling agents HATU (1.5 mmol) and DIPEA (2.5 mmol) lead to the formation of target derivatives **(pta1-**
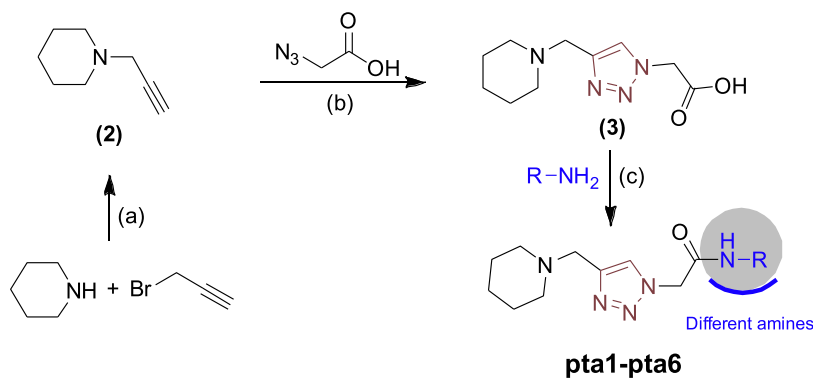
Reagents and conditions: (a) Dry Acetone, r.t, 1 min (b) Sodium ascorbate, CuSO₄.5H₂O, DMF (c) HATU, DIPEA, DMF, 50 °C.

Compound	R-NH₂ Different amines
pta1	H₂N—（phenyl）
pta2	H₂N—（benzyl）
pta3	H₂N—（tetrahydrofuran-3-yl methyl）
pta4	HN—（piperidine）
pta5	HN—O（morpholine）
pta6	HN—（pyrrolidine）

Scheme 1. Synthesis of piperidine based 1,2,3-triazolylacetamide derivatives (pta1-pta6).

pta6). Minimum amount of DMF (5–10 mL) was used as a solvent and the crude compounds were obtained by vacuum evaporating any excess DMF and precipitation in water. The crude compounds were recrystallized twice in dichloromethane: methanol solvent mixture.

N-phenyl-2-(4-(piperidin-1-ylmethyl)-1H-1,2,3-triazol-1-yl) acetamide (pta1)

Yield: 80%; Anal. Calc. For $C_{16}H_{21}N_5O$: C 64.19, H 7.07, N 23.39%; found: C 64.24, H 7.15, N 23.45%; FTIR ν_{max} cm^{-1}: 3387 (N—H), 3150 (C—H triazole ring), 2860 (C—H), 1760 (C=O), 1632 (NH); ^{1}H NMR (DMSO d_6) δ (ppm): 7.55 (1H, s, triazole ring), 7.40–7.12 (5H, m, Ar), 6.90 (1H, s, NH), 5.03 (2H, s, CH$_2$), 3.60 (2H, s, CH$_2$), 2.62 (2H, t; J = 4 Hz), 2.35 (2H, t; J = 4 Hz), 1.68–1.59 (6H, m); ^{13}C NMR (DMSO d_6) δ (ppm): 171.1 (C=O), 140.4, 136.5, 128.9, 123.7, 122.6, 121.0, 60.0, 53.7, 48.3, 23.8, 22.8; ESI-MS m/z: [M$^+$+H] 301.20; calculated: 300.18.

N-benzyl-2-(4-(piperidin-1-ylmethyl)-1H-1,2,3-triazol-1-yl) acetamide (pta2)

Yield: 80%; Anal. Calc. For $C_{17}H_{23}N_5O$: C 65.15, H 7.40, N 22.35%; found: C 65.11, H 7.46, N 22.45%; FTIR ν_{max} cm^{-1}: 3390 (N—H), 3165 (C—H triazole ring), 2865 (C—H), 1762 (C=O), 1630 (NH); ^{1}H NMR (DMSO d_6) δ (ppm): 7.55 (1H, s, triazole ring), 7.29–7.22 (5H, m, Ar), 6.18 (1H, s, NH), 4.84 (2H, s, CH$_2$), 4.54 (2H, s, CH$_2$), 3.74 (2H, s, CH$_2$), 2.69 (2H, t; J = 4 Hz), 2.41 (2H, t; J = 4 Hz), 1.69–1.60 (6H, m); ^{13}C NMR (DMSO d_6) δ (ppm): 168.4 (C=O), 142.0, 139.2, 128.7, 127.6, 126.7, 123.7, 54.5, 49.6, 48.1, 24.2, 23.4; ESI-MS m/z: [M$^+$+H] 315.20; calculated: 314.19.

2-(4-(piperidin-1-ylmethyl)-1H-1,2,3-triazol-1-yl)-N-((tetrahydrofuran-3-yl) methyl) acetamide (pta3)

Yield: 80%; Anal. Calc. For $C_{15}H_{25}N_5O_2$: C 58.61, H 8.20, N 22.78%; found: C 58.72, H 8.26, N 22.86%; FTIR ν_{max} cm^{-1}: 3392 (N—H), 3150 (C—H triazole ring), 2862 (C—H), 1765 (C=O), 1630 (NH); ^{1}H NMR (DMSO d_6) δ (ppm): 7.55 (1H, s, triazole ring), 5.36 (1H, s, NH), 4.84 (2H, s, CH$_2$), 4.49 (2H, s, CH$_2$), 3.90–3.82 (4H, m, furan ring), 3.47 (2H, dd, CH$_2$, furan ring; J = 8 Hz, 16 Hz), 3.12 (2H, dd, CH$_2$; J = 8 Hz, 16 Hz), 2.64 (2H, t; J = 4 Hz), 2.47 (1H, m, furan ring), 2.35 (2H, t; J = 4 Hz), 1.67–1.59 (6H, m); ^{13}C NMR (DMSO d_6) δ (ppm): 168.1 (C=O), 141.8, 123.6, 79.6, 67.7, 54.5, 49.0, 48.5, 43.2, 41.5, 29.7, 24.2, 23.4; ESI-MS m/z: [M$^+$+H] 309.21; calculated: 308.20.

1-(piperidin-1-yl)-2-(4-(piperidin-1-ylmethyl)-1H-1,2,3-triazol-1-yl) ethanone (pta4)

Yield: 80%; Anal. Calc. For $C_{15}H_{25}N_5O$: C 61.83, H 8.65, N 24.03%; found: C 61.74, H 8.72, N 24.13%; FTIR ν_{max} cm^{-1}: 3110 (C—H triazole ring), 2860 (C—H), 1745 (C=O); ^{1}H NMR (DMSO d_6) δ (ppm): 7.55 (1H, s, triazole ring), 4.95 (2H, s, CH$_2$), 4.44 (2H, d, CH$_2$; J = 24 Hz), 3.72 (4H, m, CH$_2$), 3.33 (2H, s, CH$_2$), 2.72 (4H, m, CH$_2$), 1.77–1.58 (10H, m); ^{13}C NMR (DMSO d_6) δ (ppm): 169.9 (C=O), 141.1, 123.2, 54.1, 49.6, 48.0, 46.7, 24.6, 23.4, 21.5; ESI-MS m/z: [M$^+$+H] 292.20; calculated: 291.21.

1-morpholino-2-(4-(piperidin-1-ylmethyl)-1H-1,2,3-triazol-1-yl) ethanone (pta5)

Yield: 80%; Anal. Calc. For $C_{14}H_{23}N_5O_2$: C 57.32, H 7.90, N 23.87%; found: C 57.45, H 7.98, N 23.75%; FTIR ν_{max} cm^{-1}: 3108

V. Srivastava, Mohmmad Younus Wani, Abdullah Saad Al-Bogami et al.

Journal of Advanced Research 29 (2021) 121–135

(C—H triazole ring), 2860 (C—H), 1745 (C=O); ^{1}H NMR (DMSO d_6) δ (ppm): 7.58 (1H, s, triazole ring), 5.08 (2H, s, CH$_2$), 3.80–3.74 (8H, m), 3.69 (2H, s, CH$_2$), 2.67–2.31 (4H, m), 1.68–1.59 (6H, m); ^{13}C NMR (DMSO d_6) δ (ppm): 169.9 (C=O), 141.1, 123.2, 54.1, 49.6, 48.0, 46.7, 24.6, 23.4, 21.5; ESI-MS m/z: [M$^+$+H] 294.18; calculated: 293.19.

2-(4-(piperidin-1-ylmethyl)-1H-1,2,3-triazol-1-yl)-1-(pyrrolidin-1-yl)ethanone (pta6)

Yield: 80%; Anal. Calc. For C$_{14}$H$_{23}$N$_5$O: C 60.62, H 8.36, N 25.25%; found: C 60.72, H 8.45, N 25.35%; FTIR ν_{max} cm^{-1}: 3105 (C—H triazole ring), 2862 (C—H), 1735 (C=O); ^{1}H NMR (DMSO d_6) (ppm): 7.83 (1H, s, triazole ring), 4.80 (2H, s, CH$_2$), 3.63 (2H, s, CH$_2$), 3.53–3.47 (4H, m), 2.68–2.58 (4H, m), 2.08–2.02 (4H, m), 1.67–1.58 (6H, m); ^{13}C NMR (DMSO d_6) δ (ppm): 171.2 (C=O), 141.8, 123.0, 54.9, 49.6, 48.2, 47.3, 25.3, 24.1, 23.2; ESI-MS m/z: [M$^+$+H] 278.20; calculated: 277.19.

Biology

25 different isolates of *C. auris* stored at −80 °C as glycerol stocks in the department were used for this study. All the isolates were previously obtained from National Institute of Communicable Diseases, and were collected with an ethics approval from Wits Human Research Ethics Committee (M140159). Prior to use, isolates were revived on Sabouraud Agar (SDA; Merck, Germany).

Inoculum preparation

All the primary cultures of *C. auris* isolates were grown in SD Broth (Merck, Germany). Post-incubation at 37 °C, broth was centrifuged and cell pellet was resuspended in normal saline solution to the cell density of $1.0–5.0 \times 10^6$ CFU/mL (0.5 McFarland Standard), which was used for all the experiments.

Antifungal susceptibility profiling

MIC and MFC values of newly synthesised piperidine based 1,2,3-triazolylacetamide derivatives (pta1-pta6) against *C. auris* strains were done according to Clinical and Laboratory Standards Institute recommended microbroth dilution assay [20]. Stock solutions of test compounds and AmB (Sigma Aldrich Co., USA) were prepared with 1% DMSO (Sigma Aldrich Co., USA) and the concentrations tested ranged from 250–0.03 µg/mL and 16–0.031 µg/mL respectively. After plates were incubated for 24 h at 37 °C, MICs were recorded visually.

For MFC determination, all the wells showing no growth were sub-cultured on SD plates and again incubated further for 24 h at 37 °C. The lowest concentration without any growth was recorded as MFC.

Determination of cell count and viability

In this study, Muse™ Cell Analyzer was used for determining the count and viability of cellular samples using the Muse™ Count and Viability assay kit as instructed by the manufacturer. Briefly, *C. auris* MRL6057 cells were inoculated in 10 mL SDB and incubated at 37 °C until mid-log phase (8 h), followed by spinning thrice at 3000 rpm for 5 min and finally inoculating cell pellet in phosphate buffer saline (PBS; Merck, Germany) containing test compounds at various concentrations (½ MIC, MIC, MFC) at 37 °C for 4 h. Both negative (untreated yeast cells) and positive controls (H$_2$O$_2$, 10 mM; Merck, Germany) were included in the study. Post-incubation cells were washed and mixed in fresh PBS, followed by mixing 20 µL of this cell suspension into 380 µL of Count & Viability reagent. The suspension was then kept for 5 min at room

temperature and thereafter examined for cell count and viability by Muse™ Cell Analyzer.

Cell membrane integrity analysis using Propidium Iodide (PI) staining

Propidium Iodide (PI; Sigma Aldrich Co., USA) was used to check *C. auris* membrane integrity, as it is commonly used as a universal marker for studying plasma membrane permeability. *C. auris* MRL6057 cells were grown in SDB for 24 h, followed by preparation of 0.5 McFarland suspension. To study the effect of test compounds, cells were subjected to test compounds at various concentrations (¼ MIC, ½ MIC and MIC) for 4 h. Both negative and positive (10 mM H$_2$O$_2$) controls were incorporated during the study. Post-exposure, cells were washed with PBS and staining procedure was performed in dark with 30 µM PI (30 min, room temperature). Thereafter, cells were washed and resuspended in PBS, followed by slide preparation for fluorescence microscopic analysis (Zeiss Microscope 780).

Protoplast preparation

For studying apoptotic markers, protoplasts of *C. auris* MRL6057 were prepared as explained previously [21]. Briefly, cells grown for 8 h were then exposed for 4 h to ¼ MIC, ½ MIC and MIC of test compounds. For the purpose of washing and resuspending yeast cells different protoplast buffers (PB) were prepared. After exposure with test compounds, cells were washed and incubated in PB-1 (1 M sorbitol, (Sigma Aldrich Co., USA), 0.05 M tris base (Merck, Germany), 0.01 M MgCl$_2$ (Sigma Aldrich Co., USA), 0.03 M DTT (Merck, Germany), pH 7.4) for 10 min at room temperature. Post-incubation, cells were harvested at 1500 rpm for 5 min and pellet was mixed and incubated in PB-2 (1 M sorbitol, 0.05 M tris base, 0.01 M MgCl$_2$, 0.001 M DTT, pH 7.4) supplemented with lyticase enzyme (1 µg/mL; Sigma Aldrich Co., USA) at room temperature for 1 h. Next, cell suspensions were centrifuged, and pellets were resuspended and incubated in PB-3 (1 M sorbitol, 0.05 M tris base, 0.01 M MgCl$_2$, pH 7.4) at room temperature for 20 min. Post-incubation cell suspension was centrifuged at 1500 rpm for 5 min and pellets with protoplasts were washed and mixed in fresh PBS and stored at 4 °C until further use.

Mitochondrial membrane depolarization assay

Change in *C. auris* mitochondrial membrane potential after exposure to test compounds was detected by using JC-10 assay kit-microplate (abcam, UK), following manufacturer's instructions. Briefly, 90 µL of *C. auris* protoplast suspensions and 50 µL JC-10 dye-loading solution was added to the designated wells of clear bottom and black walled 96-well microtiter plates (Thermo Fisher Scientific, Germany). The plates were then incubated for 1 h in dark at 37 °C, followed by the addition of 50 µL of buffer B. After incubation, protoplasts were spanned down at 800 rpm for 2 min. Fluorescence intensity was observed at Ex/Em = 490/530 nm (green fluorescence, represented as X) and 540/590 nm (red fluorescence, represented as Y) with a SpectraMax iD3 multi-mode microplate readers (Molecular Devices, USA). In apoptotic cells, the dye appears green in color as it remains in its monomeric form (Em = 530 nm) whereas, in live cells the dye aggregates in mitochondria and appear red in color (Em = 590 nm). The difference in mitochondrial membrane potential was calculated in terms of ratio of aggregates and monomeric (Y mean/X mean) form of JC-10 dye. Decrease in ratios was interpreted as mitochondrial membrane depolarization. Both negative (untreated cells) and positive (10 mM H$_2$O$_2$) controls were considered during experiments.

V. Srivastava, Mohmmad Younus Wani, Abdullah Saad Al-Bogami et al.

Journal of Advanced Research 29 (2021) 121–135

Assessment of release of cytochrome c level

The effect of compounds on release of cytochrome *c* level was studied by a method adopted from Yun and Lee, 2016 [22]. Briefly, *C. auris* MRL6057 cells (0.5 McFarland) were exposed to ¼ MIC, ½ MIC and MIC of test compounds for 4 h; negative and positive (10 mM H_2O_2) controls were taken into consideration. Post-incubation cells were washed with fresh PBS solution and were homogenized in buffer A (EDTA, 0.002 M, EDTA (Merck, Germany); Phenylmethylsulfonyl fluoride (Roche Diagnostics, Germany); 0.05 M, Tris base (pH 7.5)). Thereafter, homogenized suspension was spanned at 4000 rpm for 10 min to obtain a supernatant. The supernatant was further centrifuged for 45 min at 50,000 rpm, and the supernatant was used to measure cytosolic cytochrome *c* levels while as pellet was resuspended in buffer B (EDTA, 0.002 M; Tris base, 0.05 M; pH 5.0) to measure mitochondrial cytochrome *c* levels. The cytochrome *c* was further reduced by adding 500 mg/mL of ascorbic acid (Sigma Aldrich Co., USA) and the reduced form was relatively quantified at 550 nm by UV-1800 SHIMADZU spectrophotometer.

Annexin V-FITC/PI staining

Initial phase of apoptosis can be detected by spotting transfer of phosphatidylserine (PS) from inside to outside of cell membrane. The experiment was performed by using annexin V- FITC Apoptosis Detection Kit I (BD, USA) following company instructions. Treated *C. auris* protoplast cells (0.5 McFarland) were suspended in 1X binding buffer (available in the kit). From this 100 μL samples were aliquoted, transferred in 5 mL culture tubes and to each tube 5 μL of PI and 5 μL annexin V- FITC were added. Following addition of dyes tubes were incubated for 15 min in dark at room temperature. Thereafter, to each tube 400 μL of 1X binding buffer was mixed and samples were analyzed by BD LSRFortessa Flow cytometer (BD, USA) and results were analyzed by FlowJo_V10 software. Untreated and 10 mM H_2O_2 treated protoplasts were also included as negative and positive controls. Cell populations were divided in four different quadrants with Quadrants 1: necrosis (Annexin V$^-$/PI$^+$); Quadrants 2: late apoptosis (Annexin V$^+$/PI$^+$); Quadrants 3: early apoptosis (Annexin V$^+$/PI$^-$), Quadrants 4: live cells (Annexin V$^-$/PI$^-$).

Terminal deoxynucleotidyl transferase dUTP nick-end labeling (TUNEL) assay

To study late apoptosis in cells, DNA damage by TUNEL assay is a hallmark method and was done using *in Situ* Cell Death Detection Kit, Fluorescein (Roche Diagnostics, Germany) as directed by the supplier. Briefly, *C. auris* MRL6057 (0.5 McFarland) were subjected to ¼ MIC, ½ MIC and MIC of test compounds for 4 h along with negative (untreated yeast cells) and positive (10 mM H_2O_2) controls were considered in present experiment. After exposure, cells were washed using PBS (twice) and subsequently fixed in 4% paraformaldehyde (Sigma Aldrich Co., USA). After fixation protoplasts were prepared as described above. Protoplasts were then suspended in permeabilization solution (0.25% Triton X-100, Sigma Aldrich Co., USA), incubated for 20 min followed by rinsing with deionized water. Thereafter, slides were incubated with 50 μL TUNEL reaction mixture (450 μL label solution + 50 μL of enzyme solution) at 37 °C for 1 h (in dark) in a humidified chamber. Post-incubation samples were rinsed with deionized water and slides were observed under fluorescence microscopy (Zeiss 780) with an Ex/Em = 495/519 nm. ImageJ software was use for further image analysis.

Analysis of cell cycle arrest

The effect of test compounds on *C. auris* MRL6057 cell cycle was determined by Muse™ Cell Analyzer using Muse™ Cell Cycle kit as per instructions provided. Briefly, yeast cells were inoculated in SDB and allowed to reach mid-log phase followed by spinning at 3000 rpm for 4 min. The remaining pellet was resuspended in SDB (0.5 McFarland) and were subjected to test compounds at ¼ MIC, ½ MIC and MIC values for 4 h. After exposure, each sample was washed with fresh PBS and the pellet was fixed in 1 mL of 70% ice cold ethanol (Sigma Aldrich Co., USA) and stored at −20 °C until required. Next, 200 μL of fixed cells were aliquoted, centrifuged (3000 rpm, 5 min) and washed with sterile PBS solution. To the fixed cells, 200 μL of Muse™ Cell Cycle reagent was mixed and incubated for 30 min in dark at room temperature. The samples were examined by Muse™ Cell Analyzer. Both negative (untreated yeast cells) and positive control (10 mM H_2O_2) were also subjected to same procedure during the experiment.

Cytotoxicity studies

The test compounds were evaluated for their cytotoxic activity using horse red blood cells (NHLS, South Africa). The compounds were evaluated for their cytotoxic nature by method explained previously [21], with modifications. Briefly, 10 mL horse blood was aliquoted in 50 mL sterile falcon tubes, spinning for 10 min at 2000 rpm. Followed centrifugation, pellet was secured after spinning, washed thrice with ice-cold PBS and resuspended in chilled PBS to give 10% RBC suspension. Next, 10% RBC suspension was again diluted ten times in PBS and 100 μL of this suspension was mixed with test compounds (¼ MIC, ½ MIC, MIC and MFC). The mixture was kept for 1 h at room temperature followed by spinning for 10 min at 2000 rpm. From the supernatant, 200 μL was aliquoted and added to designated wells of a 96-well flat-bottom microtiter plate (Thermo Fisher Scientific, Germany) and at 450 nm absorbance was recorded by using SpectraMax iD3 multi-mode microplate readers (Molecular Devices, USA). Both positive (Triton X-100, 1%) and negative (fresh PBS) controls were included in the study. The result was represented in terms of percentage haemolysis (% haemolysis) and was calculated as follows:

$$\%Haemolysis = \frac{[(A450\ of\ treated\ sample) - (A450\ of\ negative\ control)]}{[(A450\ of\ positive\ control) - (A450\ of\ negative\ control)]} \times 100$$

Statistical analysis

All the data and graphs were statistically analyzed by GraphPad Prism software, version 8.0.1 using Two-way ANOVA test. Experiments were executed individually in triplicates at three different time intervals and the results were documented as means ± standard error. The statistical analysis with *p*-values ≤ 0.05 were considered significant.

Results and discussions

The outline synthesis of the target derivatives (pta1-pta6) is given in Scheme 1. 2-(4-(piperidin-1-ylmethyl)-1H-1,2,3-triazol-1-yl)acetic acid **(3)** was obtained through a click chemistry approach (Copper-Catalyzed Azide-Alkyne Cycloaddition (CuAAC)]) from 1-(prop-2-yn-1-yl)Piperidine) **(2)** and 2-azidoaceticacid. Click reactions are considered to be one of the most important green routes to the synthesis of 1,2,3-triazoles with higher reaction yields and high purity [23]. The target compounds (pta1-pta6) were obtained by treating compound **3** with different amines

V. Srivastava, Mohmmad Younus Wani, Abdullah Saad Al-Bogami et al.

Journal of Advanced Research 29 (2021) 121–135

under amide coupling conditions (see Scheme 1). The structures of all the derivatives were established by different physical and spectroscopic techniques. The structure of the triazole (3) was confirmed by FTIR, ^{1}H NMR, ^{13}C NMR and ESI MS. Presence of stretching bands at 3265 (—OH str), 2860 (C—H), 1760 (C=O) and absence of any stretching bands for azide (N=N=N at or around 2100–2160 cm^{-1}) or alkyne (around 2100–2140 cm^{-1}) indicated the cyclization of (1-(prop-2-yn-1-yl)Piperidine) (2) with 2-azidoacetic acid. The formation of the triazole ring was also confirmed by the characteristic absorption band in the region 3185–3105 cm^{-1} in the FTIR spectra due to the =C—H stretching of triazole ring. Presence of a singlet peak at 7.55–7.83 (1H, s, triazole ring) in ^{1}H NMR spectrum and the presence of peaks at 146.0 and 122.8 in ^{13}C NMR spectrum corresponding to the carbon atoms in the triazole ring established the structure of the compound 3. Positive ion mass peak at *m/z*: [M$^+$+H] 225.12 further confirmed the structure. The structures of the target compounds were also established in a similar way. The formation of the amide bonds in the target compounds was established by the characteristic stretching frequencies for C=O and N—H, represented as amide I and amide II, characteristic of amides. The ^{1}H NMR, ^{13}C NMR and ESI MS spectra were also in agreement with the established structures of the new molecules.

MIC and MFC values of compounds against C. auris isolates

Candida infection is a significant global health care threat worldwide. Emergence of MDR *C. auris* has further complicated this problem. With increasing limitation of current therapeutic regime, there is a pressing need of developing novel antifungal drugs. Various strategies and approaches have been used to handle this problem, which include the use of combination therapy, alternative approaches, semi-synthetic analogues of natural products with enhanced efficacy and structural modification of existing antifungal drugs to evade drug resistance. These approaches and strategies have helped to a great extent to fight multidrug resistant pathogens as development of a new antifungal drug has been quite challenging task, which is reflected by the fact that no new drug has been discovered after the echinocandins [24]. In this study we used the triazole scaffold, which is the core ring of azole class of antifungals and flanked it with a piperidine ring and an acetamide functionality because of their inherent biological and pharmacokinetic properties [25]. Benznidazole (N-benzyl-2-nitroimidazole-1-acetamide) is a nitroimidazole derivative containing acetamide functionality and is the drug of choice for treating infections with *Trypanosoma cruzi*.

Six novel derivatives (pta1-pta6) were obtained and tested for their antifungal efficacy against different clinical isolates of *C. auris*. MIC and MFC results reveal susceptibility of tested *C. auris* isolates towards the test compounds at varying levels. The order of potency on the basis of MIC values are pta3 > pta2 > pta1 > pta4 = pta5 = pta6 with MIC values of 0.24, 0.48, 0.97 μg/mL and >125 μg/mL, respectively (Table 1). In comparison to test compounds the MICs for AmB was found between 0.125 and 4 μg/mL. The MFC values were found to be 3.9 μg/mL, 1.95 μg/mL and 0.97 μg/mL for compounds pta1, pta2 and pta3 respectively, whereas, ≈>250 μg/mL was recorded for pta 4, pta5 and pta6. Therefore, among six test compounds, pta1, pta2 and pta3 possess low MIC values against *C. auris* isolates representing their strong anti-*Candida* activity. Similar to our results, anti-*Candida* activity of other piperidine derivatives have been reported against other *Candida* species. Ahamed and co-workers tested 14 piperidine derivatives with only two compounds exhibiting low MIC values of 0.25 μg/mL and 0.5 μg/mL against *C. albicans* [26].

Epidihydropinidine, piperidine alkaloid has been reported to have MIC values 5.37 μg/mL against non-auris *Candida* species [27]. Our results corroborate with the previous finding, suggesting that that piperidine ring containing compounds are potent inhibitors of growth and proliferation in *Candida* species. Since test compounds, pta1, pta2 and pta3 at low concentrations showed antifungal activity against *C. auris* isolates, therefore, it was worth investigating the mechanisms by which these compounds exerted antifungal activity against *C. auris* isolates. To uncover the mode of action of test compounds *C. auris* MRL6057 was used as test isolate. The rationale for selecting *C. auris* MRL 6057 isolates was its high MIC against AmB (4.0 μg/mL). Table 1 represents MIC and MFC values of test compounds and AmB against tested *C. auris* isolates.

Cell count and viability assay

Muse™ Count and Viability Assay was used for determining cell concentration and viability, which are crucial signs for healthy cell growth. The Muse™ Count & Viability reagent is a mixture of two DNA binding dyes which enables differential staining of live and dead cells. The results for cell count and viability were obtained in the form of graphs from Muse™ Cell Analyzer (Fig. 1). The graph represented both population and viability profile for *C. auris* MRL6057. In untreated negative control, 91.8% live cells were recorded whereas cells treated with H$_2$O$_2$ (positive control) resulted in 93.9% cell deaths (Fig. 1A). Treatment with test compounds (pta1, pta2 and pta3) resulted in dose dependent decrease in percentage of viable cells (Fig. 1B–D). The percent cell viability after treatment with ½ MIC, MIC and MFC values of compound pta1 was observed as 63.3%, 23.2% and 3.9% respectively. For compound pta2, percent cell viability after treatment with ½ MIC, MIC and MFC values decreased from 56.3%, 20.6% and 5.6% respectively; whereas, treatment with compound pta3 resulted in decrease from 37.0%, 16.7% and 2.2% when treated ½ MIC, MIC and MFC values, respectively. This suggest that test compounds at their corresponding MFC values completely inhibits growth and survival of *C. auris* MRL6057. These results further support our microdilution assay and validates antimycotic property of these compounds at MIC and MFC values.

Effect of compounds on C. auris cell membrane integrity

Yeast cell growth and survival is directly linked to intact plasma membrane structure as it provides a strong barrier to environmental stresses. The compounds targeting and disrupting *C. auris* plasma membrane can be considered as potential lead compounds for antifungal drug development. PI can only penetrate through disrupted cell membranes resulting in red fluorescence [28].

The effect of test compounds (pta1, pta2 and pta3) at ¼ MIC, ½ MIC and MIC on membrane integrity of *C. auris* MRL6057 was investigated by using PI. Fig. 2 represents anti-*Candida* activity of all the three compounds in a concentration dependent manner. The results revealed higher percentage of PI positive cells after exposure to test compounds, which clearly signifies disruption of plasma membrane integrity in treated yeast cells. Higher uptake of PI was observed with the increasing concentration of test compounds with a maximum uptake at MIC values followed by ½ MIC and ¼ MIC. When compared pta3 was potent disrupter of *C. auris* plasma membrane followed by pta2 and pta1.

Therefore, based on these results we hypothesized that the plasma membrane disruption after exposure to test compounds may be due to the consequence of apoptosis or necrosis in *C. auris*. Apoptosis or necrosis is a process that results in compromised plasma membrane resulting in the uptake of PI compared to health cells [28]. Therefore, these speculations were validated by studying different apoptotic parameters in *C. auris* MRL6057 isolate after exposing to these test compounds. Important apoptotic parameters, namely, mitochondrial membrane destabilization, cyto-

V. Srivastava, Mohmmad Younus Wani, Abdullah Saad Al-Bogami et al.

Journal of Advanced Research 29 (2021) 121–135

Table 1
MIC and MFC values of test compounds and AmB against *C. auris* isolates.

| *C. auris* isolates	pta1 (µg/mL)		pta2 (µg/mL)		pta3 (µg/mL)		pta4 (µg/mL)		pta5 (µg/mL)		pta6 (µg/mL)		AmB (µg/mL)	
	MIC	MFC	MIC	MFC	MIC	MFC	MIC	MFC	MIC	MFC	MIC	MFC	MIC	MFC
MRL 6326	0.48	1.95	0.24	0.97	0.12	0.48	>250	>1000	>250	>1000	>250	>1000	0.25	0.5
MRL 6183	0.48	1.95	0.24	0.97	0.12	0.48	>250	>1000	>250	>1000	>250	>1000	0.25	0.5
MRL 4888	0.97	3.9	0.48	1.95	0.24	0.97	>250	>1000	>250	>1000	>250	>1000	1.0	2.0
MRL 6015	0.48	1.95	0.24	0.97	0.12	0.48	>250	>1000	>250	>1000	>250	>1000	0.25	0.5
MRL 6333	0.97	3.9	0.48	1.95	0.24	0.97	>250	>1000	>250	>1000	>250	>1000	0.5	1.0
MRL 4587	0.97	3.9	0.48	1.95	0.24	0.97	>250	>1000	>250	>1000	>250	>1000	0.5	0.5
MRL 6334	0.97	3.9	0.48	1.95	0.24	0.97	>250	>1000	>250	>1000	>250	>1000	0.5	2.0
MRL 3785	0.48	1.95	0.24	0.97	0.12	0.48	>250	>1000	>250	>1000	>250	>1000	0.125	0.5
MRL 6059	0.97	3.9	0.48	1.95	0.24	0.97	>250	>1000	>250	>1000	>250	>1000	0.5	1.0
MRL 4000	0.97	3.9	0.48	1.95	0.24	0.97	>250	>1000	>250	>1000	>250	>1000	2.0	4.0
MRL 6065	0.97	3.9	0.48	1.95	0.24	0.97	>250	>1000	>250	>1000	>250	>1000	1.0	2.0
MRL 2921	0.97	3.9	0.48	1.95	0.24	0.97	>250	>1000	>250	>1000	>250	>1000	2.0	4.0
MRL 6125	0.48	1.95	0.24	0.97	0.12	0.48	>250	>1000	>250	>1000	>250	>1000	0.25	0.5
MRL 6338	0.48	1.95	0.24	0.97	0.12	0.48	>250	>1000	>250	>1000	>250	>1000	0.25	0.5
MRL 3499	0.97	3.9	0.48	1.95	0.24	0.97	>250	>1000	>250	>1000	>250	>1000	0.5	1.0
MRL 6194	0.48	1.95	0.24	0.97	0.12	0.48	>250	>1000	>250	>1000	>250	>1000	0.25	0.5
MRL 6005	0.97	3.9	0.48	1.95	0.24	0.97	>250	>1000	>250	>1000	>250	>1000	1.0	2.0
MRL 6057	0.97	3.9	0.48	1.95	0.24	0.97	>250	>1000	>250	>1000	>250	>1000	4.0	8.0
MRL 5762	0.97	3.9	0.48	1.95	0.24	0.97	>250	>1000	>250	>1000	>250	>1000	2.0	4.0
MRL 6173	0.48	1.95	0.24	0.97	0.12	0.48	>250	>1000	>250	>1000	>250	>1000	0.25	0.5
MRL 5765	0.97	3.9	0.48	1.95	0.24	0.97	>250	>1000	>250	>1000	>250	>1000	2.0	4.0
MRL 2397	0.97	3.9	0.48	1.95	0.24	0.97	>250	>1000	>250	>1000	>250	>1000	1.0	2.0
MRL 5418	0.97	3.9	0.48	1.95	0.24	0.97	>250	>1000	>250	>1000	>250	>1000	0.5	1.0
MRL 6277	0.97	3.9	0.48	1.95	0.24	0.97	>250	>1000	>250	>1000	>250	>1000	0.5	1.0
MRL 6339	0.97	3.9	0.48	1.95	0.24	0.97	>250	>1000	>250	>1000	>250	>1000	0.5	1.0
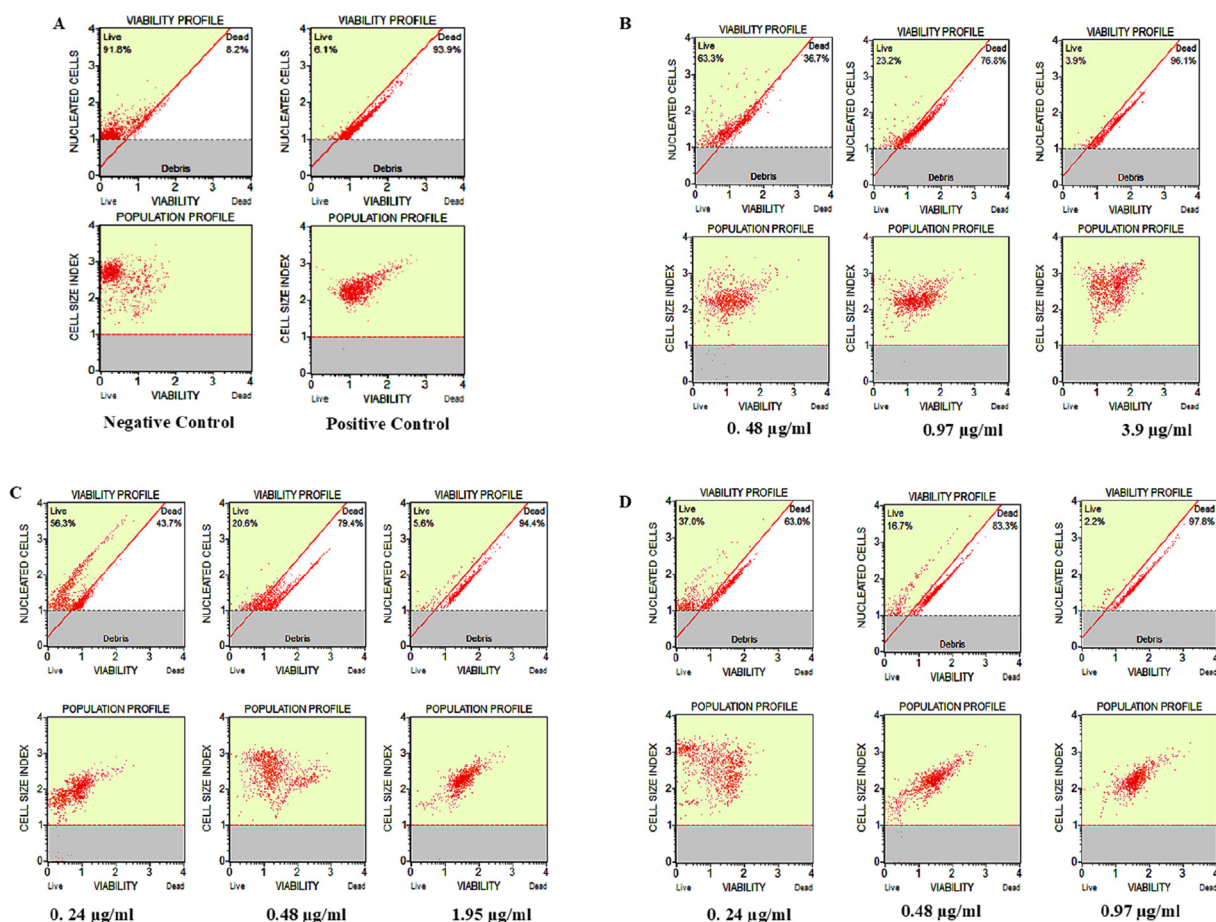
Fig. 1. Effect of test compounds on cell count and viability of *C. auris* MRL6057. Figure demonstrates viability and population profile of *C. auris* MRL6057. (A) Untreated positive control and negative control (cells treated 10 mM H_2O_2). Viability and population profile of *C. auris* after treatment with pta1 (B), pta2 (C) and pta3 (D) at different inhibitory concentrations.

V. Srivastava, Mohmmad Younus Wani, Abdullah Saad Al-Bogami et al.

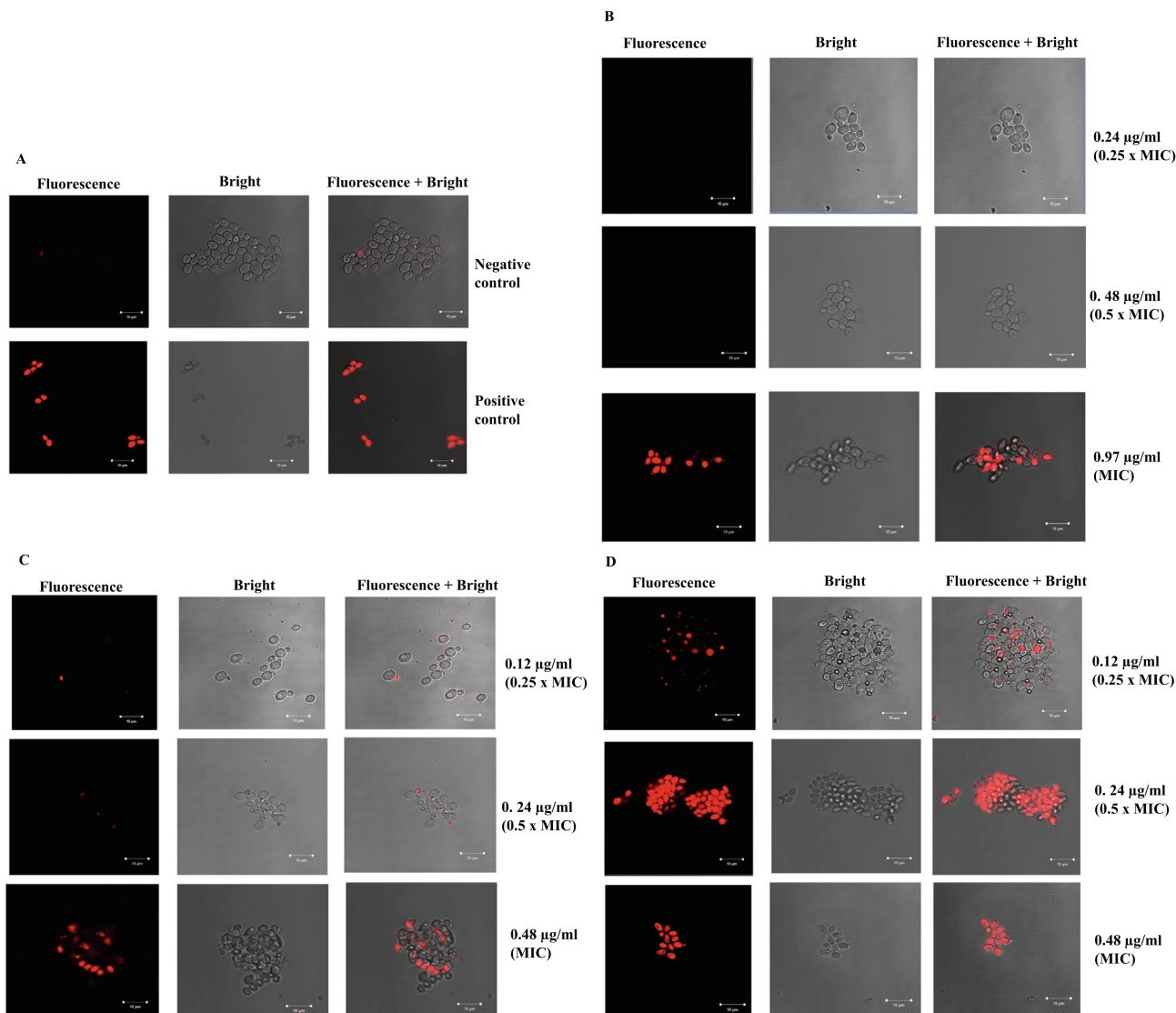*Journal of Advanced Research 29 (2021) 121–135*

Fig. 2. Uptake of PI by *C. auris* MRL 6057. Exposure of yeast cells by test compounds at various concentrations (0.25 MIC, 0.5 MIC and MIC). (A) Untreated cells were used as negative control for intact *C. auris* plasma membrane whereas, treatment with H₂O₂ caused compromised cell membrane resulting in cellular uptake of PI. (B) Exposure of *C. auris* cells to pta1; (C) exposure of *C. auris* cells to pta2 and (D) exposure of *C. auris* cells to pta3. Cells were observed by fluorescence microscopy (63x oil immersion objective).

chrome *c* discharge, exposure of phosphatidylserine and DNA impairment was investigated. Furthermore, effect of compounds on cell cycle was evaluated because cell-cycle dysregulation may lead to apoptosis due to mitotic errors [29].

Apoptosis studies

Compounds induced the loss of mitochondrial membrane potential (Δψm)

In yeasts, mitochondria besides providing metabolic energy for cell survival it is also an important role player of apoptotic pathways [30]. Therefore, it becomes important to assess whether these three test compounds have any impact over mitochondrial membrane potential, which was investigated by JC-10 dye. In the apoptosis pathway, loss of Δψm has been considered a characteristic feature. Live yeast cells have stable mitochondrial membrane potential and therefore JC-10 dye gets aggregated and produces red fluorescence, whereas in apoptotic cells Δψm is lost and thus the dye remains in its monomeric form giving a green fluorescence.

The Δψm has been calculated in terms of the ratio of JC-10 aggregates to JC-10 monomers, a reduction in the values compared to untreated control clearly indicated depolarization of mitochondrial membrane potential. Exposed *C. auris* cells showed decreased JC-10 aggregate mean fluorescence values, indicating depolarization of mitochondrial membrane. Fig. 3 shows lower ratios after treatment with test compounds (¼ MIC, ½ MIC and MIC), H₂O₂ treated cells (positive control) and compared to untreated cells (negative control). The ratio recorded for untreated cells was 1.74 whereas, 0.91 was recorded in positive control. Maximum mitochondrial depolarization was observed in case of pta3, with recorded values 1.07, 1.04 and 1.02 at concentration of ¼ MIC, ½ MIC and MIC respectively. In test compound, pta2 and pta1, the ratio varies from 1.42 to 1.05 and 1.6 to 1.24 at different concentrations respectively. These results suggest that exposure to test compounds reduced the mitochondrial membrane potential of *C. auris* isolate by collapsing the mitochondrial membrane. The mitochondrial membrane depolarization results in discharge of cytochrome *c* along with other associated factors into the cytoplasm and finally apoptosis [31]. Similar report has been published by Lemar and co-workers, where extracts of *Allium sativum* was found to exhibit
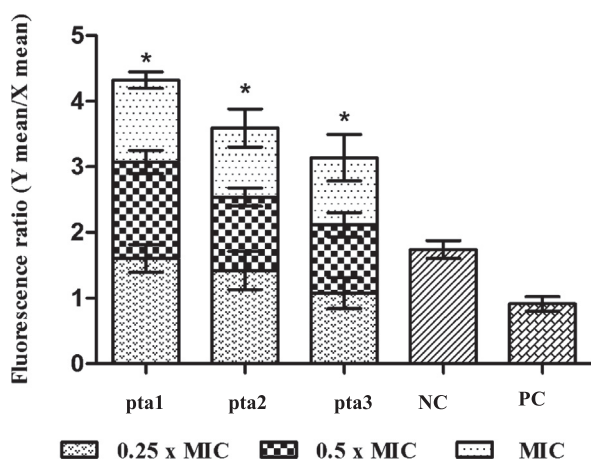
V. Srivastava, Mohmmad Younus Wani, Abdullah Saad Al-Bogami et al.

Journal of Advanced Research 29 (2021) 121–135

Fig. 3. Bar graph representing fluorescence ratio (Y mean/X mean). Y mean represents JC-10 aggregates and X mean represents JC-10 monomers. Depolarization of mitochondrial membrane was recorded in exposed *C. auris* cells in comparison to negative control.

anti-*Candida* activity [32] and its constituent diallyl disulphide (DADS) showed marked mitochondrial depolarization in *C. albicans* [33].

Apoptotic factors are activated by test compounds

In yeast cells, cytochrome *c* controls both cellular metabolism as well as apoptotic pathways [34]. It is also responsible for electron transfer from complex III to IV in mitochondria and therefore its discharge is considered as gauge for failure of electron transport chain [34]. When compared to negative control, an increase in the level of cytosolic cytochrome *c* was recorded after exposure to test compounds and H_2O_2, whereas, a decreasing trend was observed in mitochondrial cytochrome *c* level (Fig. 4A and B). Discharge of cytochrome *c* was found to be concentration dependent with a maximum release measured at MIC. With respect to untreated *C. auris* cells (negative control) where cytosolic and mitochondrial cytochrome *c* were set as 1.0, the average relative values for cytosolic and mitochondrial cytochrome *c* for H_2O_2 treated cells (positive control) were 1.37 and 0.71 respectively. Among all the three piperidine derivatives, pta3 was found to be the most potent in activating apoptotic factors in *C. auris* cells with an average relative value of 1.47 and 0.69 for cytosolic and mitochondrial cytochrome *c* followed by pta2 and pta1.

Therefore, results suggested that test compounds caused release of cytochrome *c* from the mitochondria resulting in failure of electron transport chain in *C. auris*. Hence, it can be stated that these compounds first induced depolarization of mitochondrial membrane in *C. auris* cells, which led to the bleeding of cytochrome *c* into cytosol and finally activating yeast metacaspase Yca1p (ortholog of mammalian caspases; play crucial role in yeast apoptosis). This triggers the caspase cascade mediated apoptosis in *C. auris*. This sequence of events is most commonly reported during apoptosis in yeast cell [35].

Compounds trigger PS externalisation

Phosphatidylserine is normally located in the inner side of the plasma membrane, but in apoptotic cells PS is externalised on outer side, which is considered as an early apoptosis marker in fungi [36]. Therefore, we studied PS externalisation using double staining method that employs Annexin V and PI. The exposed PS is stained by Annexin V while as PI can verifies the membrane integrity of the cells and therefore this assay can differentiate

between apoptotic, late apoptotic and necrotic cells. After treatment with different compounds (¼ MIC, ½ MIC and MIC), the number of cells (*C. auris* MRL6057) in the Q1 (Annexin V^-/PI^+) and Q2 (Annexin V^+/PI^+) quadrants has increased, whereas the number of cells in the Q3 (Annexin V^+/PI^-) and Q4 (Annexin V^-/PI^-) quadrants has decreased significantly (Fig. 5). Table 2, represents percentage of cells present in different quadrants of quadrant dot plot. In negative control (untreated cells), cell population (98.8%) was confined to Q4 representing presence of viable cells in the sample. Whereas, in positive control (cells exposed to 10 mM H_2O_2) cell population was distributed in all the quadrants (15.1%, Q1; 30.3%, Q2; 11.9% Q3 and 42.7%, Q4) suggesting exposure of 10 mM H_2O_2 mainly results in late apoptosis in *C. auris* MRL6057. Higher concentrations of test compounds resulted in higher percentage of cells confining to Q1 and Q2 whereas, a decrease in cell percentage was observed in Q3 and Q4, revealing that piperidine derivatives induced apoptosis in *C. auris*. Compound pta3 showed most potent activity with the highest percentage of cells in Q2 (97.3) and lowest concentration in Q1 (0.22), when cells were exposed to MIC values (Table 2). Similar results were recorded while analyzing effect of compounds on membrane integrity using PI as a marker, with maximum PI positive cells observed in samples exposed with pta3. Results obtained in this study are in accord with former findings where antifungal compounds were responsible for yeast cell membrane damage as well as inducing apoptosis inside *Candida* spp. Naphthofuranquinone compounds exhibited antifungal activity against azole-resistant *Candida* spp., as they exert toxicity by damaging plasma membrane, depolarization of mitochondrial membrane and DNA damage [37]. Carvacrol, a monoterpene phenol, resulted in plasma membrane depolarization associated with apoptosis and DNA fragmentation in *C. albicans* [38]. Synthetic MCh-AMP1, a peptide was reported to damage plasma membrane by increasing its permeability, inducing potassium leakage and ROS production in *C. albicans* [39].

Therefore, these results reveal that inhibition of growth and survival of *C. auris* by test compounds was a result of induced apoptosis. In Annexin V/PI double staining, early apoptosis is shown by cells that were exposed to sub-inhibitory concentration, while a late apoptosis was depicted at higher concentrations of test compounds.

DNA damage in C. auris

DNA fragmentation, which is an important outcome of apoptosis in yeast cells was investigated by TUNEL assay. This assay measures DNA damage by binding to free 3'-OH ends of cleaved DNA [40,33]. *C. auris* MRL6057 cells exposed to test compounds and H_2O_2 represented an increased number of green fluorescence dots (TUNEL$^+$ nuclei) as compared to untreated negative cells, indicating DNA damage in yeast cells (Fig. 6). With increasing concentration of test compounds, both number as well as intensity of green fluorescence increased, revealing the concentration dependent effect. Results revealed that pta3 was most active against *C. auris* cells as it exerted DNA damage even at sub-MICs, followed by pta2 and pta1. Therefore, our results strongly support that the test compounds caused apoptotic DNA damage, a marker of late stage apoptosis in yeast cells.

Further, TUNNEL assay corroborates the apoptotic nature of these three compounds against *C. auris* cells and the observations are in accord with previous literature, where researchers have documented dose dependent effect of natural compounds on induction of apoptosis and DNA damage in *Candida* cells [41,42]. These findings are also in agreement with our research findings where semi-synthetic compounds were reported to cause dose dependent late apoptosis in *C. albicans* [5,21].
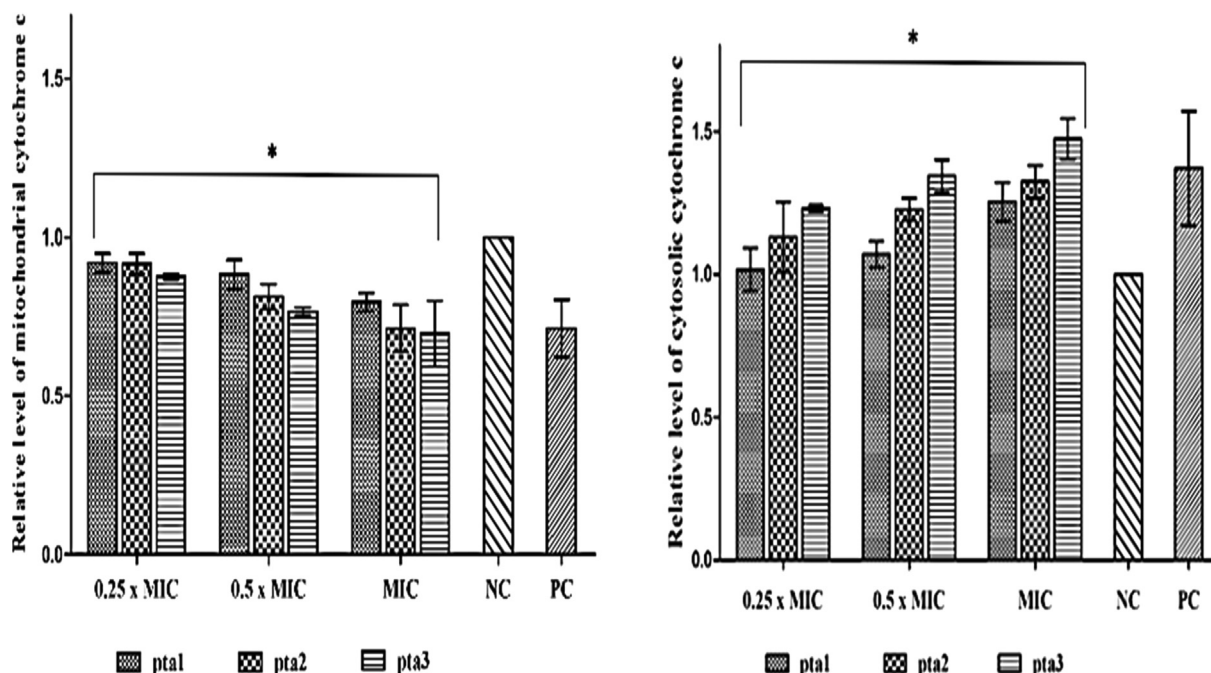
Fig. 4. Activation of apoptotic factors in *C. auris* MRL6057 in presence of test compounds and H_2O_2. Mitochondrial (A) and cytosolic (B) cytochrome *c* were estimated at 550 nm. Results show decreased cytochrome *c* level in mitochondria whereas increased cytochrome *c* level in cytosol. NC: negative control; PC: positive control.

Cell cycle arrest in C. auris

As exposure of test compounds resulted in DNA damage in yeast cells and it is well reported that damaged DNA cannot enter cell cycle for prevention of mutations. Therefore, we studied the cell cycle arrest in *C. auris* cells after exposure to test compounds. In negative control (untreated cells) around 87.6% cells were in G0/G1 phase followed by 6.5% and 5.4% in S phase and G2/M phase, respectively. Exposure of *C. auris* MRL6057 cells to test compounds resulted in cell cycle arrest at different phases (Fig. 7). Exposure of cells to sub-inhibitory concentrations of pta1 (¼ MIC and ½ MIC) and pta2 (¼ MIC) had no effect over *C. auris* cell cycle and was similar to negative control. However, at MIC value of pta1 a new trend was observed in which 58.85% cells were in G0/G1 phase, 24.6% cells in S phase and 15.8% cells were in G2/M phase. Compound pta2 at ½ MIC also impacted normal cell cycle of *C. auris* with 71.45%, 18.05% and 10.1% cells accumulated in G0/G1 phase, S phase and G2/M phase respectively. Furthermore, at MIC value the percentage of cells was decreased in G0/G1 phase (32%) and increased in S phase (44.85%) and G2/M phase (22.75%). Exposure to pta3 at different inhibitory concentrations ceased the cell cycle in S phase which was evident from presence of large population of cells in S phase with 48.75% cells (¼ MIC); 59% cells (½ MIC) and 67.55% cells (MIC). The cell percentage in G2/M phase was low (11.45% cells reported at ¼ MIC; 12.7% cells reported at ½ MIC and 13.7% cells reported at MIC) as compared to G0/G1 phase (39.25% cells reported at ¼ MIC; 26.55% cells reported at ½ MIC and 18.35% cells reported at MIC). Altogether, the results revealed that all three test compounds allowed the cells to proceed through G0/G1 and caused a cell arrest in S phase. Compound pta3 has most prominent effect on cell cycle progression in *C. auris* and even at low concentration (¼ MIC) cells were arrested in S phase, urthermore, the percentage of arrested cells in S phase was increased with increasing concentration of compound.

It has been reported that piperidines and their derivatives have DNA binding/cleavage activity in eukaryotes and are potential anticancer agents [43]. Furthermore, these heterocyclic compounds are well known for generation of Reactive Oxygen Species (ROS) and ROS-dependent apoptosis, mitochondrial membrane depolarization, and expression of caspase which is a marker for both intrinsic and extrinsic apoptosis in malignant cells [44,45]. In *Saccharomyces cerevisiae*, apoptosis is reported to be induced due to damaged DNA [46]. Cells are highly vulnerable to DNA damage in the course of S-phase of cell cycle because in this phase DNA is replicated. Any impairment in DNA or disruption in DNA replication is responded by activation of surveillance pathways known as checkpoint controls that results in cell cycle arrest and thus bargain time for repair before restarting the cycle [47]. In yeast, there are two surveillance networks, namely, DNA replication checkpoint and DNA damage checkpoint that are being operated during S-phase and these pathways are conserved in yeast. Therefore, any replicative stress and DNA damage encountered by yeast triggers activation of Mec1 and Rad53 kinases, responsible for this checkpoint control [48,49]. The activation of these checkpoints results in cell cycle arrest in S-phase. Krishnan and co-workers (2007) [47], have discussed cell cycle arrest in yeast by 2-methyl-1,8 epoxy naphthalimide (ENA), a DNA-binding compound that arrest cell cycle in S-phase. Other DNA-interacting compounds with cytotoxic properties are, for example, bleomycin, which is known for inhibition of DNA synthesis [50]; carboplatin, forms adduct with DNA [50]; oxaliplatin forms complex with DNA [51]; and cyclophosphamide, crosslinks and results in breakage of DNA strands [51]. These compounds are involved in DNA damage and inhibit synthesis of DNA and thereby induce cellular apoptosis. Additionally, Klassen and co-worker (2005) discussed about *Pichia acaciae* toxin that showed activation of DNA-damaging checkpoints, arrest cells in S-phase and induce apoptosis in *S. cerevisiae* [52]. According to Weinberger and co-workers (2005), mutations that results in disconnecting DNA replication from the ongoing cell cycle by obstructing checkpoint controlling system dependent on DNA replication forks and detaining consequent cell cycle events are responsible for ROS induction, Yca1p stimulation and simultaneously triggering the Rad53p-dependent response to DNA damage. All these consecutive events finally lead to apoptosis in yeast cells [46].
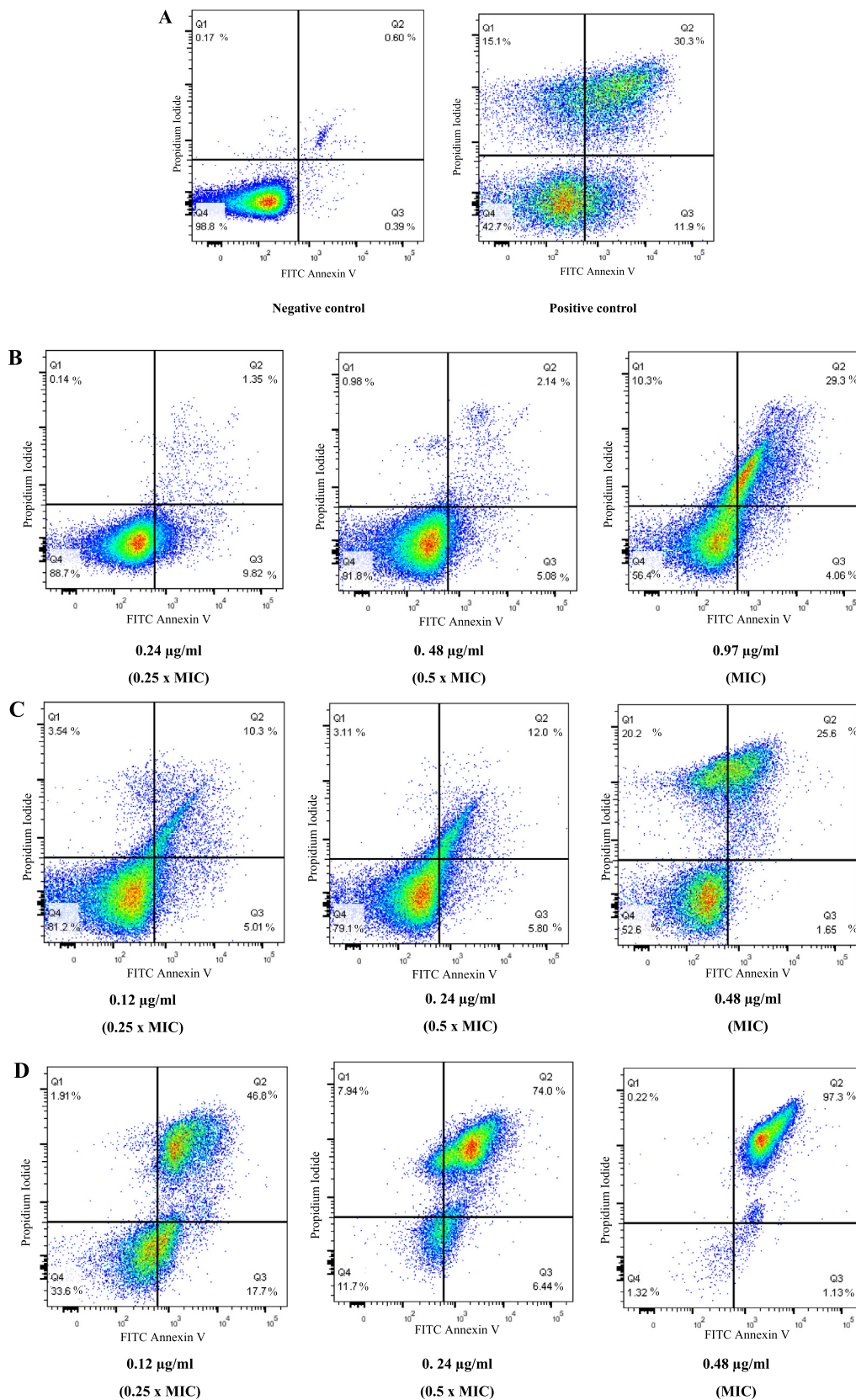
Fig. 5. Flow cytometric analysis of PS exposure using AnnexinV/PI double staining. *C. auris* cells were treated with different concentrations of test compounds. (A) Untreated cells were considered as negative control whereas H_2O_2 (10 mM) was added for positive control. Cells exposed to pta1 (B), pta2 (C) and pta3 (D).

Table 2
Percentage of cells present in different quadrants (Q1–Q4) of quadrant dot plot. Q1: necrosis (Annexin V$^-$/PI$^+$), Q2: late apoptosis (Annexin V$^+$/PI$^+$), Q3: early apoptosis (Annexin V$^+$/PI$^-$) and Q4: viable cells (Annexin V$^-$/PI$^-$).

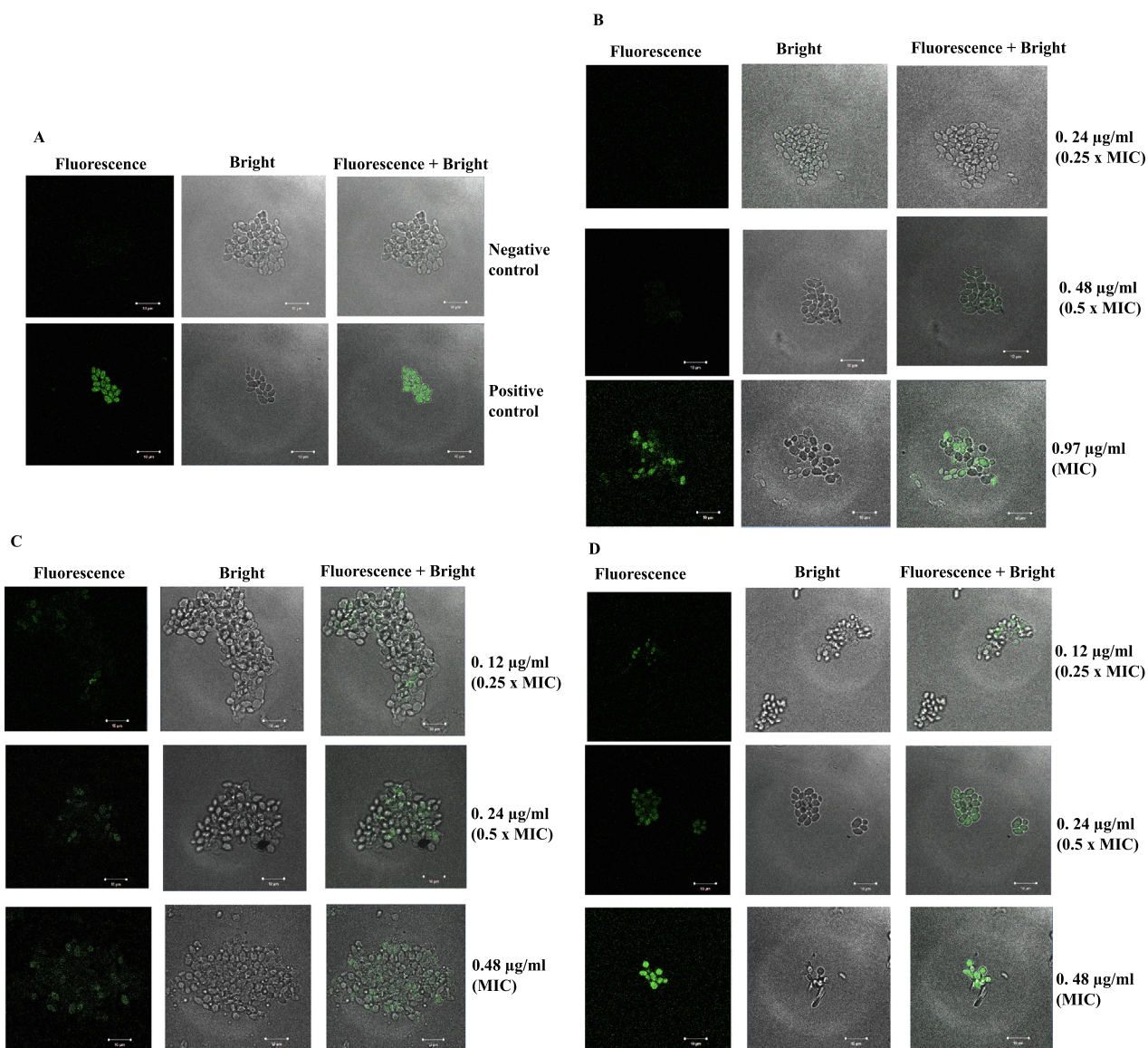| Test compounds	Quadrants	0.25 × MIC (% cells)	0.5 × MIC (% cells)	MIC (% cells)
pta1	Q1	0.14	0.98	10.3
	Q2	1.35	2.14	29.3
	Q3	9.82	5.08	4.06
	Q4	88.7	91.8	56.4
pta2	Q1	3.54	3.11	20.2
	Q2	10.3	12.0	25.6
	Q3	5.01	5.8	1.65
	Q4	81.2	79.1	52.6
pta3	Q1	1.91	7.94	0.22
	Q2	46.8	74	97.3
	Q3	17.7	6.44	1.13
	Q4	33.6	11.7	1.32
Positive control	Q1	15.1		
	Q2	30.3		
	Q3	11.9		
	Q4	42.7		
Negative control	Q1	0.17		
	Q2	0.60		
	Q3	0.39		
	Q4	98.8		

Fig. 6. Confocal scanning fluorescence images of C. auris MRL 6057 cells. (A) Untreated cells were considered as negative control whereas, treatment with H$_2$O$_2$ (10 mM) was positive control. Cells exposed to pta1 (B), pta2 (C) and pta3 (D).

V. Srivastava, Mohmmad Younus Wani, Abdullah Saad Al-Bogami et al.

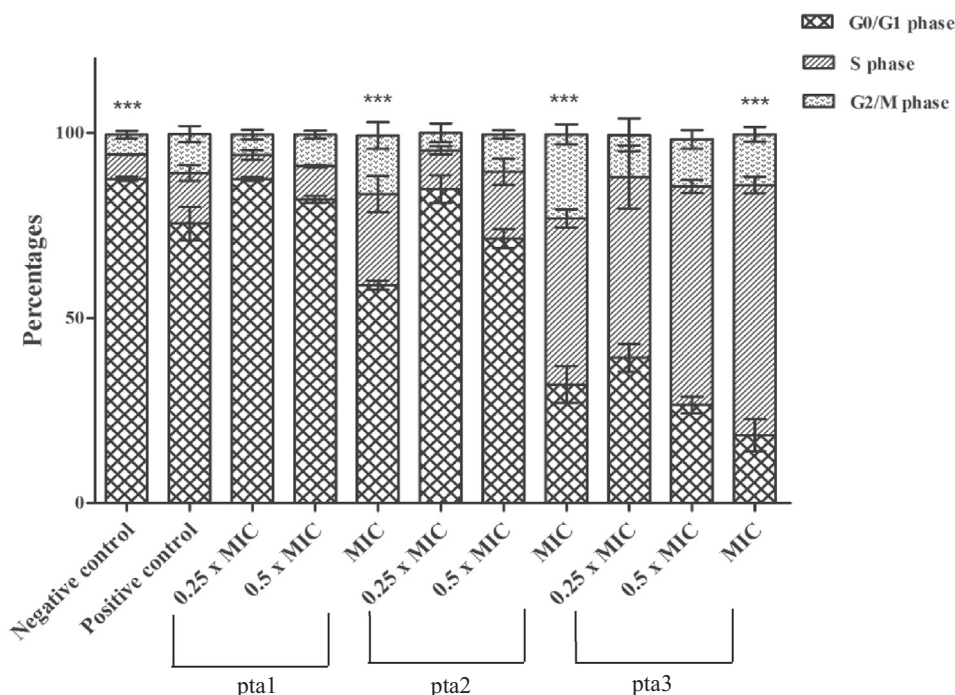*Journal of Advanced Research 29 (2021) 121–135*

Fig. 7. Cell cycle analysis of *C. auris* by Muse™ Cell Analyzer. Figure showing effect of test compounds (at different concentrations) on cell cycle progression in *C. auris* MRL6057. Untreated yeast cell were considered as negative control.
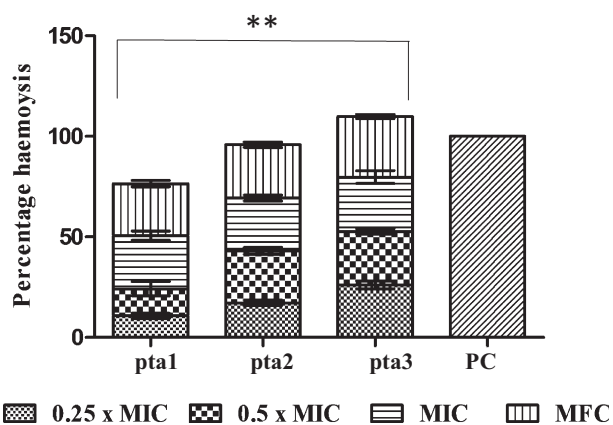

Fig. 8. Haemolytic activity of test compounds. Test compounds at different inhibitory concentrations exhibited significantly low RBCs lysis when compared with positive control (reference for 100% haemolysis). No haemolysis was observed in negative control (PBS).

In present study it is likely that exposure of test piperidine based compounds in *C. auris* cells causes DNA damage and impairment of DNA replication that results in blocking cell cycle in S-phase. During this phase, test compound treated yeast cells were reported TUNEL-positive, indicating DNA fragmentation. In addition, as indicated by AnnexinV/PI staining, cells exposed PS at the outer membrane face was increased. We also recorded decreased mitochondrial membrane potential and bleeding of cytochrome *c* from mitochondria to cytosol. Our results suggest that test compounds cause DNA damage and impaired DNA replication that in turn induces cellular apoptosis in *C. auris* cells.

Haemolytic activity of test compounds

Currently used antifungal drugs have high toxicity and this complicates their usage in immunodeficient individuals. Therefore,

there is an indispensable need to develop new antifungal drugs that are highly specific and result in targeted cell death without harming patients. Since, test compounds (pta1, pta2 and pta3) showed significant anti-*Candida* potential and were able to trigger cellular apoptosis in *C. auris* isolates, therefore, toxicity determination of these compounds was very important. Cytotoxicity assay was performed on horse RBCs. The percent haemolysis in positive control was 100% whereas, there was no lysis in negative control. When compared to controls the test compounds showed some haemolysis, ranging from 10.75% to 30.09% (Fig. 8). Haemolysis displayed by pta1 was 10.75%, 13.49%, 26.38% and 25.87% for ¼ MIC, ½ MIC, MIC and MFC respectively. Compound pta2 resulted in 17.23%, 25.86%, 26.17% and 26.56% for ¼ MIC, ½ MIC, MIC and MFC respectively. Whereas, pta3 was found to show 26.15%, 26.53%, 27.06% and 30.09% for ¼ MIC, ½ MIC, MIC and MFC respectively. These results confirmed that these compounds were considerably less toxic in comparison to positive control, and thereby signified the use of these compounds for future *in vivo* studies and thereby providing a potential candidate for antifungal drug development.

Conclusion

Our results demonstrated that the piperidine based triazolylacetamide derivatives (pta1, pta2 and pta3) showed potent antifungal activity against MDR *C. auris* isolates. The compounds were capable of arresting cell cycle in S-phase, which was directly linked to DNA damage. The compounds also exhibited dose-dependent effect on crucial yeast apoptotic markers, such as, mitochondrial membrane potential, movement of cytochrome *c* from mitochondria to cytosol, PS externalization and DNA damage. Among three compounds, pta3 was established to be the most potent compound. In addition, hemolytic assay indicated low cytotoxic effect of these compounds. In conclusion, these compounds with their DNA damaging and induction of cellular apoptosis mechanisms have potential to be taken to next levels of studies in developing novel antifungal drugs.

V. Srivastava, Mohmmad Younus Wani, Abdullah Saad Al-Bogami et al.

Journal of Advanced Research 29 (2021) 121–135

Author contributions

AA MYW ASA conceived and designed research, VS MYW conducted experiments, VS MYW AA analysed results, VS MYW wrote the manuscript. All authors read and approved the manuscript.

Compliance with Ethics Requirements

All procedures followed were in accordance with the ethical standards of the responsible committee on human experimentation (institutional and national) and with the Helsinki Declaration of 1975, as revised in 2008 (5). Informed consent was obtained from all patients for being included in the study.

Prior using the Candida isolates for the research work, ethical approval was obtained from Human Research Ethics Committee of University of the Witwatersrand (M140159).

Declaration of Competing Interest

The authors declare that they have no known competing financial interests or personal relationships that could have appeared to influence the work reported in this paper.

Acknowledgement and Funding

Appendix A. Supplementary material

Supplementary data to this article can be found online at https://doi.org/10.1016/j.jare.2020.11.002.

References:

[1] Lone SA, Ahmad A. *Candida auris*-the growing menace to global health. Mycoses 2019;62:620–37. doi: https://doi.org/10.1111/myc.12904.

[2] Govender NP, Magobo RE, Mpembe R, Mhlanga M, Matlapeng P, Corcoran C, et al. *Candida auris* in South Africa, 2012–2016. Emerg Infect Dis 2018;24:2036–40. doi: https://doi.org/10.3201/eid2411.180368.

[3] Chowdhary A, Prakash A, Sharma C, Kordalewska M, Kumar A, Sarma S, et al. A multicentre study of antifungal susceptibility patterns among 350 *Candida auris* isolates (2009–17) in India: role of the ERG11 and FKS1 genes in azole and echinocandin resistance. J Antimicrob Chemother 2018;73:891–9. doi: https://doi.org/10.1093/jac/dkx480.

[4] Gintjee TJ, Donnelley MA, Thompson 3rd GR. Aspiring antifungals: review of current antifungal pipeline developments. J Fungi 2020;6:28. doi: https://doi.org/10.3390/jof6010028.

[5] Wani MY, Ahmad A, Aqlan FM, Al-Bogami AS. Azole based acetohydrazide derivatives of cinnamaldehyde target and kill *Candida albicans* by causing cellular apoptosis. ACS Med Chem Lett 2020;11:566–74. doi: https://doi.org/10.1021/acsmedchemlett.0c00030.

[6] Lass-Flörl C. Triazole antifungal agents in invasive fungal infections. Drugs 2011;71:2405–19. doi: https://doi.org/10.2165/11596540-000000000-00000.

[7] Peyton LR, Gallagher S, Hashemzadeh M. Triazole antifungals: a review. Drugs Today (Barc) 2015;51:705–18. doi: https://doi.org/10.1358/dot.2015.51.12.2421058.

[8] Vardanyan R. Piperidine-based drug discovery. Elsevier; 2017.

[9] Pizzuti MG, Minnaard AJ, Feringa BL. Catalytic asymmetric synthesis of the alkaloid (+)-myrtine. Organic Biomolecular Chem 2008;6:3464–6. doi: https://doi.org/10.1039/B807575A.

[10] Aeluri R, Alla M, Bommena VR, Murthy R, Jain N. Synthesis and antiproliferative activity of polysubstituted tetrahydropyridine and piperidin-4-one-3-carboxylate derivatives. Asian J Organic Chem 2012;1:71–9. doi: https://doi.org/10.1002/ajoc.201200010.

[11] Bozorov K, Zhao J, Aisa HA. 1,2,3-Triazole-containing hybrids as leads in medicinal chemistry: a recent overview. Bioorg Med Chem 2019;27:3511–31. doi: https://doi.org/10.1016/j.bmc.2019.07.005.

[12] Akbar I, Ahamed A, Arif IA, Kumar RS, Selva K, Mailal A. Synthesis of novel pyridine-connected piperidine and 2H-thiopyran derivatives and their larvicidal, nematicidal, and antimicrobial activities. J Mex Chem Soc 2018;62. doi: https://doi.org/10.29356/jmcs.v62i4.472.

[13] Wieczorek D, Kwasniewska D, Hsu L-H, Shen T-L, Chen Y-L. Antifungal activity of morpholine and piperidine based surfactants. Tenside Surfactants Detergents 2020;57:104–8. doi: https://doi.org/10.3139/113.110667

[14] Ku-Lung H, Katsunori T, Jae WC, Landon RW, Anna ES, Holly P, et al. Discovery and optimization of piperidyl-1,2,3-triazole ureas as potent, selective, and in vivo-active inhibitors of α/β-hydrolase domain containing 6 (ABHD6). J Med Chem 2013;56:8270–9.

[15] Ku-Lung H, Katsunori T, Landon RW, Anna ES, Holly P, Jordon I, et al. Development and optimization of piperidyl-1,2,3-triazole ureas as selective chemical probes of endocannabinoid biosynthesis. J Med Chem 2013;56:8257–69.

[16] Jaiprakash NS, Devanand BS. Synthesis of some novel 3-(1-(1-substitutedpiperidin-4-yl)-1H-1,2,3-triazol-4-yl)-5-substituted phenyl-1,2,4-oxadiazoles as antifungal agents. Eur J Med Chem 2011;46:1040–4.

[17] Jaiprakash NS, Rahul RN, Devanand BS. Synthesis of novel 3-(1-substituted piperidin-4-yl)-1H-1,2,3-triazol-4-yl)-1,2,4-oxadiazol-5(4H)-one as antifungal agents. Bioorg Med Chem Lett 2009;19(13):3564–7.

[18] Kashmiri L, Kaushik CP, Krishan K, Ashwani K, Asif KQ, Abid H, et al. One-pot synthesis and cytotoxic evaluation of amide-linked 1,4-disubstituted 1,2,3-bistriazoles. Med Chem Res 2014;23:4761–70.

[19] Kashmiri L, Nisha P, Poonam R, Ashwani K, Anil K. Design, synthesis, antimicrobial evaluation and docking studies of urea-triazole-amide hybrids. J Mol Struct 2020;1215:128234.

[20] Clinical and Laboratory Standards Institute. Reference method for broth dilution antifungal susceptibility testing of yeasts-Third Edition: Approved Standard M27-A3. CLSI, Wayne, PA, USA; 2008.

[21] Lone SA, Wani MY, Fru P, Ahmad A. Cellular apoptosis and necrosis as therapeutic targets for novel eugenol tosylate congeners against *Candida albicans*. Sci Rep 2020;10:1191. doi: https://doi.org/10.1038/s41598-020-58256-4.

[22] Yun DG, Lee DG. Silibinin triggers yeast apoptosis related to mitochondrial Ca^{2+} influx in *Candida albicans*. Int J Biochem Cell Biol 2016;80:1–9. doi: https://doi.org/10.1016/j.biocel.2016.09.008.

[23] Sandip GA, Suleman RM, Vandana SP. Click chemistry: 1,2,3-triazoles as pharmacophores. Chemistry: Asian J 2011;6:2696–718.

[24] Butts A, Krysan DJ. Antifungal drug discovery: something old and something new. PLoS Pathog 2012;8(9):. doi: https://doi.org/10.1371/journal.ppat.1002870e1002870.

[25] Kennedy Jr GL. Biological effects of acetamide, formamide, and their monomethyl and dimethyl derivatives. Crit Rev Toxicol 1986;17:129–82. doi: https://doi.org/10.3109/10408448609023768.

[26] Ahamed A, Arif IA, Kumar RS, Idhayadhulla A, Keerthana SR, Manilal A. Synthesis of novel pyridine-connected piperidine and 2H-thiopyran derivatives and their larvicidal, nematicidal, and antimicrobial activities. J Mex Chem Soc 2018;62. doi: https://doi.org/10.29356/jmcs.v62i4.472.

[27] Fyhrquist P, Virjamo V, Hiltunen E, Julkunen-Tiitto R. Fitoterapia, Epidihydropinidine, the main piperidine alkaloid compound of Norway spruce (Picea abies) shows promising antibacterial and anti-Candida activity. Fitoterapia 2017;117:138–46. doi: https://doi.org/10.1016/j.fitote.2017.01.011.

[28] Setiawati S, Nuryastuti T, Ngatidjan N, Mustofa M, Jumina J, Fitriastuti D. In vitro antifungal activity of (1)-N-2-Methoxybenzyl-1,10-phenanthrolinium bromide against *Candida albicans* and its effects on membrane integrity. Mycobiology 2017;45:25–30. doi: https://doi.org/10.5941/MYCO.2017.45.1.25.

[29] Azzopardi M, Farrugia G, Balzan R. Cell-cycle involvement in autophagy and apoptosis in yeast. Mech Ageing Dev 2017;161:211–24. doi: https://doi.org/10.1016/j.mad.2016.07.006.

[30] Akbar M, Essa MM, Daradkeh G, Abdelmegeed MA, Choi Y, Mahmood L, et al. Mitochondrial dysfunction and cell death in neurodegenerative diseases through nitroxidative stress. Brain Res 2016;1637:34–55. doi: https://doi.org/10.1016/j.brainres.2016.02.016.

[31] Simon HU, Haj-Yehia A, Levi-Schaffer F. Role of reactive oxygen species (ROS) in apoptosis induction. Apoptosis 2000;5:415–8. doi: https://doi.org/10.1023/A:1009616228304.

[32] Lemar KM, Passa O, Aon MA, et al. Allyl alcohol and garlic (Allium sativum) extract produce oxidative stress in *Candida albicans*. Microbiology (Reading) 2005;151:3257–65. doi: https://doi.org/10.1099/mic.0.28095-0.

[33] Lemar KM, Aon MA, Cortassa S, O'Rourke B, Muller CT, Lloyd D. Diallyl disulphide depletes glutathione in *Candida albicans*: oxidative stress-mediated cell death studied by two-photon microscopy. Yeast 2007;24:695–706. doi: https://doi.org/10.1002/yea.1503.

[34] Huttemann M, Pecina P, Rainbolt M, Sanderson TH, Kagan VE, Samavati L, et al. The multiple functions of cytochrome c and their regulation in life and death decisions of the mammalian cell: from respiration to apoptosis. Mitochondrion 2011;11:369–81. doi: https://doi.org/10.1016/j.mito.2011.01.010.

[35] Adrain C, Martin SJ. The mitochondrial apoptosome: a killer unleashed by the cytochrome seas. Trends Biochem Sci 2001;26:390–7. doi: https://doi.org/10.1016/s0968-0004(01)01844-8.

[36] Jia C, Zhang J, Yu L, Wang C, Yang Y, Rong X, et al. Antifungal activity of coumarin against *Candida albicans* is related to apoptosis. Front Cell Infect Microbiol 2019;8:445. doi: https://doi.org/10.3389/fcimb.2018.00445.

[37] Neto JBA, da Silva CR, Neta MAS, Campos RS, Siebra JT, Silva RAC, et al. Antifungal activity of Naphthoquinoidal compounds in vitro against fluconazole-resistant strains of different *Candida* species: a special emphasis on mechanisms of action on *Candida tropicalis*. PLoS ONE 2014;9:. doi: https://doi.org/10.1371/journal.pone.0093698e93698.

V. Srivastava, Mohmmad Younus Wani, Abdullah Saad Al-Bogami et al.

Journal of Advanced Research 29 (2021) 121–135

[38] Niu C, Wang C, Yang Y, Chen R, Zhang J, Chen H, et al. Carvacrol induces *Candida albicans* apoptosis associated with Ca2+/calcineurin pathway. Front Cell Infect Microbiol 2020;10:192. doi: https://doi.org/10.3389/fcimb.2020.00192.

[39] Seyedjavadi SS, Khani S, Eslamifar A, Ajdary S, Goudarzi M, Halabian R, et al. The antifungal peptide MCh-AMP1 derived from Matricaria chamomilla inhibits *Candida albicans* growth via inducing ROS generation and altering fungal cell membrane permeability. Front Microbiol 2020;10:3150. doi: https://doi.org/10.3389/fmicb.2019.03150.

[40] Higuchi Y. Chromosomal DNA fragmentation in apoptosis and necrosis induced by oxidative stress. Biochem Pharmacol 2003;66:1527–35. doi: https://doi.org/10.1016/s0006-2952(03)00508-2.

[41] Shirtliff ME, Krom BP, Meijering RA, Peters BM, Zhu J, Scheper MA, et al. Farnesol-induced apoptosis in *Candida albicans*. Antimicrob Agents Chemother 2009;53:2392–401. doi: https://doi.org/10.1128/AAC.01551-08.

[42] Khan A, Ahmad A, Khan LA, Manzoor N. *Ocimum sanctum* (L.) essential oil and its lead molecules induce apoptosis in *Candida albicans*. Res Microbiol 2014;165:411–9. doi: https://doi.org/10.1016/j.resmic.2014.05.031.

[43] Zuravka I, Roesmann R, Sosic A, Wende W, Pingoud A, Gatto B, et al. Synthesis and DNA cleavage activity of Bis-3-chloropiperidines as alkylating agents. Chem Med Chem 2014;9:2178–85. doi: https://doi.org/10.1002/cmdc.201400034.

[44] Arun A, Ansari MI, Popli P, Jaiswal S, Mishra AK, Dwivedi A, et al. New piperidine derivative DTPEP acts as dual-acting anti-breast cancer agent by targeting ER α and downregulating PI 3K/Akt-PKC α leading to caspase-dependent apoptosis. CellProlif 2018;51:. doi: https://doi.org/10.1111/cpr.12501e12501.

[45] Gobec M, Obreza A, Prijatelj M, Brus B, Gobec S, Mlinaric-Rascan I. Selective cytotoxicity of amidinopiperidine based compounds towards Burkitt's lymphoma cells involves proteasome inhibition. PLoS One 2012;7:. doi: https://doi.org/10.1371/journal.pone.0041961e41961.

[46] Weinberger M, Ramachandran L, Feng L, Sharma K, Sun X, et al. Apoptosis in budding yeast caused by defects in initiation of DNA replication. J Cell Sci 2005;118:3543–53. doi: https://doi.org/10.1242/jcs.02477.

[47] Krishnan V, Dirick L, Lim HH, Lim TSJ, Si-Hoe SL, Cheng CS, et al. A novel cell cycle inhibitor stalls replication forks and activates S phase checkpoint. Cell Cycle 2007;6:1621–30. doi: https://doi.org/10.4161/cc.6.13.4373.

[48] Longhese MP, Clerici M, Lucchini G. The S phase checkpoint and its regulation in Saccharomyces cerevisiae. Mut Res 2003;532:41–58. doi: https://doi.org/10.1016/j.mrfmmm.2003.08.009.

[49] Osborn AJ, Elledge SJ, Zou L. Checking on the fork: The DNA-replication stress-response pathway. Trends Cell Biol 2002;12:509–16. doi: https://doi.org/10.1016/s0962-8924(02)02380-2.

[50] Hurley LH. DNA and its associated processes as targets for cancer therapy. Nat Rev Cancer 2002;2:188–200. 110.1038/nrc749.

[51] Nelson SM, Ferguson LR, Denny WA. DNA and the chromosomes-varied targets for chemotherapy. Cell Chromosomes 2004;3:2. doi: https://doi.org/10.1186/1475-9268-3-2.

[52] Klassen R, Meinhardt F. Induction of DNA damage and apoptosis in *Saccharomyces cerevisiae* by a yeast killer toxin. CellMicrobiol 2005;7:393–401. doi: https://doi.org/10.1111/j.1462-5822.2004.00469.x.